Weierstraß-Institut
für Angewandte Analysis und Stochastik

Leibniz-Institut im Forschungsverbund Berlin e. V.

Preprint ISSN 2198-5855

Non-local and local temporal cavity soliton interaction in delay models of mode-locked lasers

Andrei G. Vladimirov

submitted: November 26, 2021

Weierstrass Institute
Mohrenstr. 39
10117 Berlin
Germany
E-Mail: andrei.vladimirov@wias-berlin.de

No. 2894
Berlin 2021

2020 *Mathematics Subject Classification.* 78A60, 37N20, 78M35.

2010 *Physics and Astronomy Classification Scheme.* 42.65.-k, 42.65.Re, 42.60.Fc, 42.65.Sf, 42.65.Tg.

Key words and phrases. Mode-locking, nonlinear mirror, delay differential equation model, cavity solitons.

The support by the Deutsche Forschungsgemeinschaft (DFG-RSF project No. 445430311) is gratefully acknowledged. The author is thankful to D. Turaev, S. Yanchuk, and D. Rachinskii for useful discussions.

Edited by
Weierstraß-Institut für Angewandte Analysis und Stochastik (WIAS)
Leibniz-Institut im Forschungsverbund Berlin e. V.
Mohrenstraße 39
10117 Berlin
Germany

Fax: +49 30 20372-303
E-Mail: preprint@wias-berlin.de
World Wide Web: http://www.wias-berlin.de/

Non-local and local temporal cavity soliton interaction in delay models of mode-locked lasers

Andrei G. Vladimirov

Abstract

Interaction equations governing slow time evolution of the coordinates and phases of two interacting temporal cavity solitons in a delay differential equation model of a nonlinear mirror mode-locked laser are derived and analyzed. It is shown that non-local pulse interaction due to gain depletion and recovery can lead either to a development of harmonic mode-locking regime, or to a formation of closely packed incoherent soliton bound state with weakly oscillating intersoliton time separation. Local interaction via electric field tails can result in an anti-phase or in-phase stationary or breathing harmonic mode-locking regime.

Temporal cavity solitons (TCSs) are short pulses of light circulating in optical resonators. These solitons were detected experimentally in driven fiber cavities [15] and optical microcavities for frequency comb generation [9, 11]. Another optical system which can support TCSs is a mode-locked (ML) laser (see [6] and references therein) used for short optical pulse generation. Only those pulses, however, that are localized in time on a scale much smaller than the cavity round trip time, can be interpreted as TCSs. In particular, in monolithic semiconductor ML lasers, where the gain relaxation time is larger than the cavity round trip time, self-starting ML pulses have a long gain recovery tail and therefore cannot be considered as localized. On the contrary, when the cavity round trip time is sufficiently large as compared to the gain relaxation time the pulses emitted by a passively ML external cavity semiconductor laser can be transformed into TCSs [17]. Note, however, that cavity solitons can also appear in Haus master equation models of ML fiber lasers where gain is so slow that it can be considered as constant within the cavity round trip time, see e. g. [7, 19, 22].

Being well separated from one another TCSs can interact via their exponentially decaying tails. Their interaction in ML lasers was studied in a number of publications using experimental, numerical and combined analytical and numerical tools [1, 2, 6, 12, 13, 16, 20–22, 31]. Many of these studies were performed within the framework of the mean-field Haus master equations for the case where the gain was either adiabatically eliminated or constant in time. The effect of the gain (and/or absorption) saturation and recovery on the pulse interaction in ML lasers was investigated in [1, 3, 10, 13, 18, 22, 25, 33]. In particular, it was shown using a phenomenological approach that the gain depletion and subsequent recovery can result in repulsive pulse interaction leading to formation of harmonic mode-locking (HML) with equally spaced pulses [13]. A similar result was obtained in [3, 18] using the delay differential (DDE) model of a passively ML laser developed in [28–30].

Here using an approach different from that of Ref. [18] the interaction of TCSs is studied in a DDE model of nonlinear optical loop mirror - nonlinear amplifying loop mirror (NOLM-NALM) ML laser with arbitrary gain relaxation time proposed in [26] (see also Ref. [25] for the model with adiabatically eliminated gain). Unlike Haus master equations, DDE models of ML lasers do not assume small gain and loss per cavity round trip, which means that ML pulses in these models are always asymmetric. Depending on the ratio of the spectral filtering width and the gain relaxation rate two types of TCS interaction are considered, which are referred below as non-local and local TCS interaction. For both

DOI 10.20347/WIAS.PREPRINT.2894 Berlin 2021

these types of interaction the equations governing the slow evolution of the time coordinates and phases of the interacting solitons are derived. It is shown that apart from the repulsion non-local TCS interaction due to gain depletion and recovery an attractive interaction is also possible, which can lead to a closely packed "incoherent" oscillating TCS bound state. Local TCS interaction via electric field component can lead to a formation of HML regimes with fixed phase difference between the interacting TCSs as well as breathing HML regimes. The analytical results obtained here can be used to study the TCS interaction in the model of passively ML laser [29] and other DDE ML laser models.

A NOLM-NALM ML laser also known as figure-of-eight laser contains a main cavity with gain medium coupled to a bidirectional nonlinear mirror loop with intensity dependent reflectivity. Let us consider the DDE laser model of a NOLM-NALM laser developed in [26] using the lumped element approach described in [28–30]:

$$\partial_t A + (\Gamma + i\omega) A = \Gamma\sqrt{\kappa} e^{\frac{1-i\alpha}{2} g_\tau + i\theta} \mathcal{R}\left(|A_\tau|^2\right) A_\tau, \tag{1}$$

$$\gamma^{-1}\partial_t g = p - g - \left(e^g - 1\right)|A|^2 \left|\mathcal{R}\left(|A|^2\right)\right|^2. \tag{2}$$

Here $A(t)$ is the electric field envelope, $g(t)$ is the cumulative gain, Γ – is the normalized bandwidth of the spectral filter, κ is the linear round-trip attenuation factor, α is the linewidth extension factor, γ is the normalized gain relaxation rate, p is the pump parameter, and $\theta = \theta_0 - \omega\tau$ is a phase shift and ω is the reference frequency, which will be chosen below. The subscript τ denotes delayed argument, where the delay time τ is equal to the dimensionless cold cavity round trip time. Complex reflectivity of the nonlinear mirror is defined by the relation:

$$\mathcal{R}\left(|A|^2\right) = \sqrt{G}\left[(1-K)\, e^{-i\chi(1-K)|A|^2} - K e^{-i\chi KG|A|^2}\right],$$

where $0 < K < 1$ is the splitting ratio, $G < 1$ ($G > 1$) is the linear attenuation (amplification) in the nonlinear mirror loop, and χ is the normalized Kerr coefficient. In particular, $K = 0.5$ corresponds to a symmetric splitter. The quantity $|\mathcal{R}|^2$ in Eq. (2) is the intensity reflectivity of the nonlinear mirror [4, 5, 14]. This quantity oscillates with the intensity between the minimal value $|\mathcal{R}|^2 = G(1-2K)^2$ and the maximal value $|\mathcal{R}|^2 = G$, where the first minimum is achieved at $|A|^2 = 0$ and corresponds to zero reflectivity $|\mathcal{R}|^2 = 0$ in the case of symmetric splitter, $K = 0.5$.

Linear stability of the trivial solution of Eqs. (1) and (2), $A = 0$ and $g = p$, is determined by the equation

$$\partial_t A + (\Gamma + i\omega) A = \Gamma\sqrt{\kappa} e^{\frac{1-i\alpha}{2} p + i\theta - i\omega\tau} \mathcal{R}(0) A_\tau, \tag{3}$$

giving an infinite set of eigenvalues that can be expressed in terms of the Lambert function:

$$\lambda = -\Gamma - i\omega + \frac{1}{\tau} W_k\left[\Gamma\tau\sqrt{\kappa}\mathcal{R}(0)\, e^{\Gamma\tau + \frac{1-i\alpha}{2} p + i\theta}\right] \tag{4}$$

with $k = 0, \pm 1 \pm 2 \ldots$. Real parts of these eigenvalues for $-10 \le k \le 10$ are shown in Fig. 1(a) as functions of the splitting ratio K. It is seen that the trivial solution is stable when K is sufficiently close to 0.5. In particular, the real parts of all the eigenvalues tend to $-\infty$ for $K \to 0.5$, except for a single eigenvalue $\lambda_0 \to -(\Gamma + i\omega)$. Therefore, the use of almost symmetric beam splitter is needed to achieve the TCS regime in Eqs. (1) and (2).

In order to derive the interaction equations governing the slow evolution of the time coordinates and phases of two well separated interacting TCSs let us first rewrite the model equations (1) and (2) in a more general form:

$$\partial_t \mathbf{U} = \mathbf{F}(\mathbf{U}) + \mathbf{H}(\mathbf{U}_\tau), \tag{5}$$

where the column vector $\mathbf{U} = \begin{pmatrix} \Re A & \Im A & z \end{pmatrix}^T$, $z = g - p$, $\mathbf{F}(0) = \mathbf{H}(0) = 0$, and subscript τ denotes time delay. Furthermore, in our case similarly to the DDE ML laser model in [29] only two first components of the vector $\mathbf{H}$ are nonzero, see Eqs. (1) and (2).

Let us assume that the cavity round trip is sufficiently large, $\tau \gg \Gamma^{-1}, \gamma^{-1}$ and consider τ_0-periodic TCS solution of Eq. (5) defined by $\mathbf{U} = \mathbf{u}_0$ and $\omega = \omega_0$, where $\mathbf{u}_0(t) = \mathbf{u}_0(t + \tau_0)$ with $\mathbf{u}_0 = \begin{pmatrix} \Re A_0 & \Im A_0 & z_0 \end{pmatrix}^T$, ω_0 is the frequency shift, and the period τ_0 is close to the delay time τ.

The decay rates of the TCS tails are determined by the linear equation (3), where the delay time τ and the frequency offset ω are replaced with $-\delta = \tau - \tau_0$ and ω_0, respectively [25, 32], and the linearization of Eq. (2) on the trivial solution:

$$\partial_t A + (\Gamma + i\omega_0) A = \Gamma\sqrt{\kappa} e^{\frac{1-i\alpha}{2}p + i\theta + i\omega_0\delta} \mathcal{R}(0) A_{-\delta}, \tag{6}$$

$$\partial_t z = -\gamma z. \tag{7}$$

Equation (7) assumes that the decay rate of the TCS tail at $t \to \infty$ is determined by the eigenvalue $-\gamma$, while Eq. (6) has an infinite number of eigenvalues defined by Eq. (4), where τ and ω are replaced with $-\delta$ and ω_0, respectively. However, in the limit $K \to 0.5$, where $\mathcal{R}(0) \to 0$, only a single linear eigenvalue $-(\Gamma + i\omega_0)$ with negative real part remains, while the real parts of all the other eigenvalues tend to $+\infty$. Hence, in this limit the leading edge of the TCS decays faster than exponentially [25], whereas the field component of the trailing edge of the TCS contains only a single decaying exponent. Therefore, in a laser with symmetric beam splitter the TCS asymptotical behavior at sufficiently large positive times $t > 0$ is described by:

$$A_0 \sim a e^{-(\Gamma + i\omega_0)t}, \quad z_0 \sim b e^{-\gamma t}. \tag{8}$$

Here $a(b)$ is complex (real) coefficient, which depends on the particular form of the pulse solution and can be calculated numerically. Since the leading edge of the pulse decays faster than exponentially it can be neglected when constructing the interaction equations. Note, that in Eq. (8) it is assumed that the pulse is positioned at the origin of the coordinate t. In the case where $\Gamma > \gamma$, the gain tail behind the TCS is longer than the tail of the electromagnetic field and well separated TCSs interact via their gain components. Below this type of interaction will be referred to as “non-local” interaction. When, on the other hand, $\Gamma < \gamma$ the gain tail is shorter than the field tail and the TCSs interact via the field components. This second type of interaction will be further referred to as “local” interaction. Local interaction can take place, in particular, when the gain variable is eliminated adiabatically [25]. Note, that a small asymmetry of the splitter does not change the analytical results presented below and only slightly modifies the decay rate of the TCS trailing tail. Sufficiently large asymmetry on the other hand can destabilize the trivial solution [26] thus breaking a necessary condition of the TCS formation.

Linear stability of the TCS solution $\mathbf{U} = \mathbf{u}_0$ is determined by linearizing Eq. (5) on this solution and calculating the spectrum of the resulting linear operator $\mathcal{L}$. Due to the translational and phase shift symmetries of the model equations, $A(t) \to A(t - t_0)$ and $A(t) \to A(t)e^{i\phi_0}$ with arbitrary constant t_0 and ϕ_0, the operator $\mathcal{L}$ has a double zero eigenvalue, $\mathcal{L}\mathbf{v}^{(\tau,\phi)} = 0$, where the translational and phase shift neutral (Goldstone) modes are $\mathbf{v}^{(\tau)} = \partial_t \mathbf{u}_0^{(\tau)}$ and $\mathbf{v}^{(\phi)} = \begin{pmatrix} -\Im A_0 & \Re A_0 & 0 \end{pmatrix}^T$, respectively. Let us assume that the TCS is stable, which means that the rest of the spectrum of $\mathcal{L}$ lies in the left half of the complex plane. Similarly, the adjoint operator $\mathcal{L}^\dagger$ has a double zero eigenvalue associated with the so-called adjoint neutral modes $\mathbf{w}^{(\tau,\phi)}$, $\mathcal{L}^\dagger \mathbf{w}^{(\tau,\phi)} = 0$. Since the adjoint operator $\mathcal{L}^\dagger$ is obtained from $\mathcal{L}$ by the transformations including the time reversal, $t \to -t$ (see Appendix A), the asymptotic behavior of the adjoint neutral modes at sufficiently large negative times $t < 0$ is given

by

$$\xi^{(\tau,\phi)} \sim c^{(\tau,\phi)} e^{(\Gamma - i\omega_0)t}, \quad \zeta_g^{(\tau,\phi)} \sim d^{(\tau,\phi)} e^{\gamma t}, \tag{9}$$

where the adjoint neural mode is given by the row vector $\mathbf{w}^{(\tau,\phi)} = \begin{pmatrix} \Re\xi^{(\tau,\phi)} & \Im\xi^{(\tau,\phi)} & \zeta_g^{(\tau,\phi)} \end{pmatrix}$ and $c^{(\tau,\phi)}$ ($d^{(\tau,\phi)}$) is a complex (real) coefficient, which can be calculated numerically. Similarly to the leading tail of the TCS solution, the trailing tail of the adjoint neutral mode decays faster than exponentially at $t > 0$. The adjoint neutral modes are assumed to satisfy the bi-orthogonality condition: $\int_0^{\tau_0} \mathbf{w}^{(j)} \cdot \mathbf{v}^{(k)} dt = \delta_{jk}$ with $j, k = \tau, \phi$.

Let us look for the solution of Eq. (5) in the form of a sum of two well separated TCSs

$$\mathbf{U} = \mathbf{u}_\Sigma + \delta\mathbf{u}, \quad \mathbf{u}_\Sigma = \mathbf{u}_1 + \mathbf{u}_2, \tag{10}$$

where $\mathbf{u}_{1,2} = \begin{pmatrix} \Re A_{1,2} & \Im A_{1,2} & g_{1,2} \end{pmatrix}^T$ with $A_{1,2} = A_0\left(t - \tau_{1,2}\right) e^{i\phi_{1,2}}$ and $g_{1,2} = z_0\left(t - \tau_{1,2}\right)$, plus a small correction $\delta\mathbf{u} = \mathcal{O}\left(\epsilon\right)$. Here the small parameter ϵ characterizes the weak overlap of the TCSs. Coordinates $\tau_{1,2}$ and phases $\phi_{1,2}$ of the interacting TCSs are assumed to be slow functions of time, $\partial_t\tau_{1,2}, \partial_t\phi_{1,2} = \mathcal{O}\left(\epsilon\right)$.

Substituting Eq. (10) into Eq. (5), collecting the first order terms in small parameter ϵ, and using the solvability conditions [8] yields

$$\partial_t\tau_{1,2} = -\left\langle \mathbf{w}_{1,2}^{(\tau)} \mathbf{P} \right\rangle, \quad \partial_t\phi_{1,2} = \left\langle \mathbf{w}_{1,2}^{(\phi)} \mathbf{P} \right\rangle, \tag{11}$$

$$\mathbf{P} = -\partial_t\mathbf{u}_\Sigma + \mathbf{F}\left(\mathbf{u}_\Sigma\right) + \mathbf{G}\left[\mathbf{u}_\Sigma\left(t - \tau\right)\right], \tag{12}$$

where $\left\langle \cdot \right\rangle = \int_0^{\tau_0} \cdot dt$, $\mathbf{w}_{1,2}^{(\tau,\phi)} = \begin{pmatrix} \Re\xi_{1,2}^{(\tau,\phi)} & \Im\xi_{1,2}^{(\tau,\phi)} & \zeta_{1,2}^{(\tau,\phi)} \end{pmatrix}$ with $\xi_{1,2}^{(\tau,\phi)} = \xi^{(\tau,\phi)}\left(t - \tau_{1,2}\right) e^{-i\phi_{1,2}}$ and $\zeta_{1,2}^{(\tau,\phi)} = \zeta^{(\tau,\phi)}\left(t - \tau_{1,2}\right)$. Similarly to the case of dissipative soliton interaction in partial differential equations models , the right hand side (RHS) of the interaction equations (11) can be expressed in terms of the TCS solution itself and the adjoint neutral modes, see, e.g. [23, 24, 27]. The details of the calculations are given in the Appendix A. As a result, the interaction equations for τ_0-periodic TCS take the form

$$\partial_t\tau_{1,2} = \pm\mathbf{w}_{1,2}^{(\tau)}\left(0\right)\mathbf{u}_{2,1}\left(0\right) \mp \mathbf{w}_{1,2}^{(\tau)}\left(\frac{\tau_0}{2}\right)\mathbf{u}_{2,1}\left(\frac{\tau_0}{2}\right), \tag{13}$$

$$\partial_t\phi_{1,2} = \mp\mathbf{w}_{1,2}^{(\phi)}\left(0\right)\mathbf{u}_{2,1}\left(0\right) \pm \mathbf{w}_{1,2}^{(\phi)}\left(\frac{\tau_0}{2}\right)\mathbf{u}_{2,1}\left(\frac{\tau_0}{2}\right), \tag{14}$$

where without the loss of generality one can assume that $t = 0$ and $t = \tau_0/2$ correspond respectively to the middle point between two TCS and the opposite point on a circle with the circumference τ_0, see Fig. 1. Note that due to the super-exponential decay of the TCS leading and adjoint neutral modes trailing tails the terms $\mathbf{w}_1^{(\tau,\phi)}\left(0\right)\mathbf{u}_2\left(0\right)$ and $\mathbf{w}_2^{(\tau,\phi)}\left(\tau_0/2\right)\mathbf{u}_1\left(\tau_0/2\right)$ in Eqs. (13) and (14) can be neglected. The remaining terms $\mathbf{w}_2^{(\tau,\phi)}\left(0\right)\mathbf{u}_1\left(0\right)$ and $\mathbf{w}_1^{(\tau,\phi)}\left(\tau_0/2\right)\mathbf{u}_2\left(\tau_0/2\right)$ entering the RHS of the equations for $\tau_2(\phi_2)$ and $\tau_1(\phi_1)$ respectively, have very different magnitudes except for the case where the TCSs are close to equidistant in the cavity, $\Delta = \tau_2 - \tau_1 \approx \tau_0/2$. This means that except for this case the TCS interaction is strongly asymmetric and does not satisfy third Newton's law [3, 24].

Let us first consider the case of non-local interaction, $\Gamma > \gamma$. Here the gain component of the trailing tail of the TCS decays slower than the field component and, hence, TCSs interact via the gain tail behind the pulse. This interaction will be called non-local interaction since the gain tail can last much longer than the tail of the electromagnetic field component. Therefore, when the time separation of two TCSs is sufficiently large the terms proportional to $e^{-\Gamma t}(e^{\Gamma t})$ in the asymptotic expressions (8)

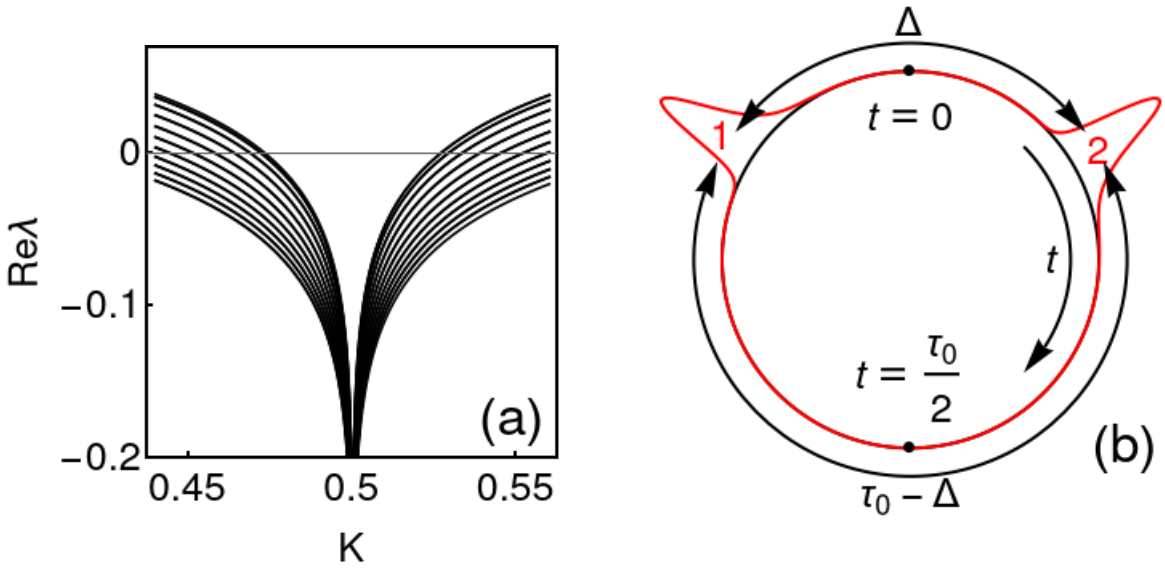

Figure 1: Largest real parts of the eigenvalues λ defined by Eq. (4) (a). Schematic representation of two interacting TCSs labeled as 1 and 2 (b). Δ is the TCS time separation and τ_0 is the TCS period.

and (9) for the TCS and adjoint neutral modes can be neglected. Then substituting these asymptotic expressions into Eqs. (13) and (14) yields

$$\partial_t \Delta = -s^{(\tau)} \left[e^{-\gamma \Delta} - e^{-\gamma(\tau_0 - \Delta)} \right], \tag{15}$$

$$\partial_t \psi = s^{(\phi)} \left[e^{-\gamma \Delta} - e^{-\gamma(\tau_0 - \Delta)} \right], \tag{16}$$

where $\Delta = \tau_2 - \tau_1$ and $\psi = \phi_2 - \phi_1$ are the TCS time separation and phase difference, $s^{(\tau,\phi)} = bd^{(\tau,\phi)}$. The interaction equations (15) and (16) have a single stationary solution corresponding to a HML regime with two equidistant pulses in the cavity, $\Delta\tau = \tau_0/2$. This solution is stable for $s^{(\tau)} < 0$ and unstable for $s^{(\tau)} > 0$. The first case corresponds to the repulsion of two TCSs on a circle when the distance between them is increasing until the pulses become equidistant. In the second case two TCS are attracted to one another.

Figure 2(a) illustrates the evolution of the TCS coordinates with the round trip number calculated by numerical integration of the model equations (1) and (2). In this figure corresponding to positive $s^{(\tau)} = 0.432$ and $s^{(\phi)} = -3.531$ the first TCS attracts the second one until the distance between them becomes sufficiently small and a closely packed bound state of two TCS is formed. The intensity time trace of this bound state is shown in Fig. 3(a) where the peak power of the first TCS is larger than that of the second one. Similar bound states were observed experimentally in a NOLM-NALM figure-of-eight ML laser in [12]. Fig. 3(b) obtained by numerical integration of the model equations (1) and (2) illustrates how the TCS phase difference ψ and time separation Δ evolve with the cavity round trip number. It is seen that similarly to the “type-A” bound states reported in a Haus model of passively ML laser with a slow absorber [22] the phase difference ψ grows monotonously in time. Therefore, this bound state can be called “incoherent.” Furthermore, it is seen that the TCS time separation Δ is in fact not stationary, but exhibits small amplitude oscillations with the period equal to the time interval during which ψ changes by 2π. This indicates that the oscillations of Δ are due to local interaction of the TCSs via exponentially decaying tails of the electromagnetic field. Note that since the dependence of ψ on time is not strictly linear [see Fig. 3(b)], the time-averaged local interaction force between the two TCSs can be nonzero. Note, however, that the approach based on the properties of the unperturbed TCS solutions and their adjoint neutral modes is hardly applicable to describe the bound state shown

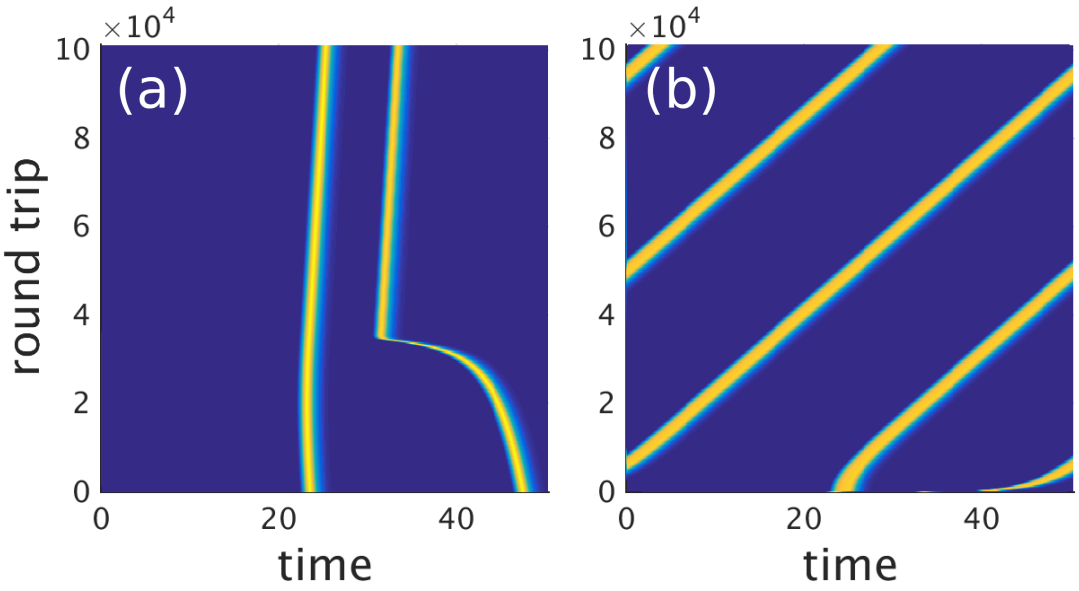

Figure 2: Interaction of two TCSs leading to a closely packed incoherent TCS bound state at $p = 5.5$ (a) and a stable HML with two equidistant pulses circulating in the laser cavity at $p = 5.7$ (b). Other parameters are: $T = 50.$, $\Gamma = 1$, $\kappa = 0.8$, $\alpha = 0$, $\gamma = 0.3$, $G = 0.5$, $\chi = 2$.

in Fig. 3(a), where the peak power of the second interacting TCS is noticeably smaller than that of the first one.

Figure 2(b) corresponds to the case of negative $s^{(\tau)} = -2.643$ leading to TCS repulsion and $s^{(\phi)} = -3.599$. In this figure the second TCS is repelled from the first one until the two TCS become equidistant in time, which corresponds to a HML regime with two pulses per cavity round trip.

In the case where $\Gamma < \gamma$ the gain tail behind the pulse is shorter than that of the electric field. In this case the field component dominates the interaction of well separated TCS and the interaction equations take the form:

$$\partial_t \Delta = -\Re\left[q^{(\tau)} f\left(\Delta, \psi\right)\right], \quad \partial_t \psi = \Re\left[q^{(\phi)} f\left(\Delta, \psi\right)\right], \tag{17}$$

$$f\left(\Delta, \psi\right) = e^{-(\Gamma + i\omega_0)\Delta - i\psi} - e^{-(\Gamma + i\omega_0)(\tau_0 - \Delta) + i\psi}, \tag{18}$$

where $q^{(\tau,\phi)} = a\bar{c}^{(\tau,\phi)}$ and bar denotes complex conjugation. These equations have two steady states with equal pulse separations, $\Delta = \tau_0/2$, and opposite phase differences, $\psi = 0$ and $\psi = \pi$, on the interval $\psi \in [0, 2\pi)$. They correspond to HML regimes with equidistant in time in-phase and anti-phase TCSs. Due to the symmetry property of Eqs. (17) and (18), $t \to -t$ and $\psi \to \psi + \pi$, if one of the two steady states is asymptotically stable, another is unstable, and vice versa. Furthermore, Eqs. (17) and (18) can exhibit an Andronov-Hopf bifurcation at $\Re\left\{\left[q^{(\tau)}\left(\Gamma + i\omega_0\right) - iq^{(\phi)}\right] e^{-i\omega_0\tau_0/2}\right\} = 0$, where a pair of limit cycles of opposite stability (stable and unstable) bifurcate simultaneously from the in-phase and anti-phase steady states. These two cycles are shown in Fig. 5(a) for the parameter values of Fig. 4, which correspond to $q^{(\tau)} = -9.386 + 10.312i$, $q^{(\phi)} = 5.870 - 16.291i$, and $\omega_0 = 0.183427$. It is seen that in agreement with the results of numerical simulations shown in Fig. 4 two stable attractors, fixed point with $\psi = \pi$ and a stable limit circle born from the fixed point with $\psi = 0$, coexist in the phase plane of the interaction equations. With the increase of the pump parameter p limit cycles shown in Fig. 5(a) shrink and disappear in the inverse Andronov-Hopf bifurcations of the corresponding fixed points. This bifurcation stabilizes (destabilizes) the fixed point with $\psi = 0$ ($\psi = \pi$). The resulting phase portrait of Eqs. (17) and (18) with $q^{(\tau)} = -19.633 + 7.608i$, $q^{(\phi)} = 17.251 -$

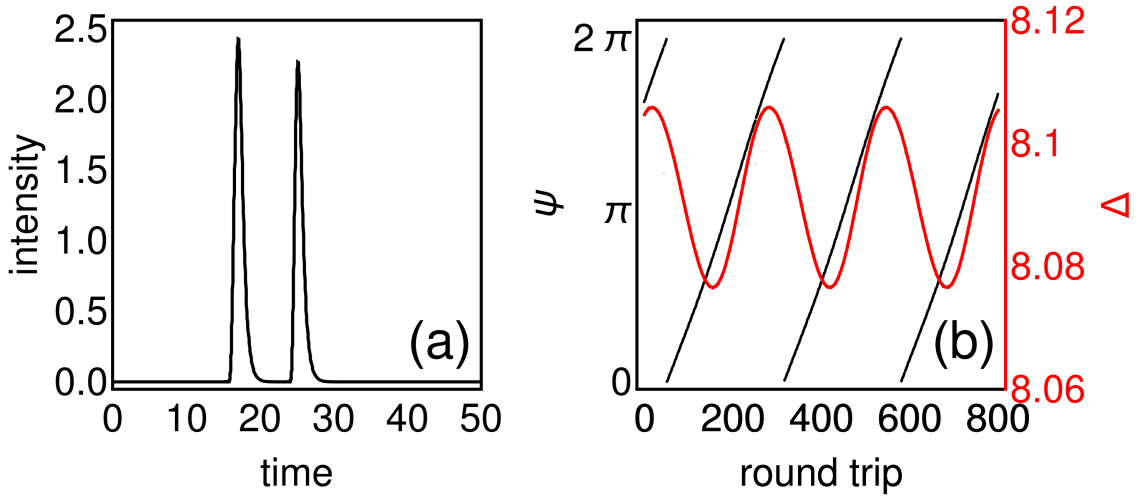

Figure 3: Intensity time trace of the closely packed TCS bound state (a); intersoliton phase difference ψ and time separation Δ of this bound state as a functions of round trip number (b). Parameters are the same as for Fig. 2(a).

$11.001i$, and $\omega_0 = 0.181633$ calculated numerically for $p = 7.2$ is shown in Fig. 5(b). This figure is in agreement with the direct numerical simulations of the model equations (1) and (2) which indicate that a stable HML regime with two in-phase pulses is formed as a result of the local TCS interaction at $p = 7.2$. Note, that in a laser with sufficiently broad spectral filtering width Γ local interaction of the pulses can be too weak against the background noise. Therefore a laser with relatively narrow spectral filter bandwidth generating sufficiently broad pulses is required for experimental observation of the local TCS interaction leading to HML regimes.

To conclude, the interaction equations governing the time evolution of the coordinates and phases of locally and non-locally interacting TCSs in a ML NOLM-NALM laser have been derived. It has been shown that in the case of non-local TCSs interaction due gain depletion and slow recovery apart from the usual repulsion leading to the development of HML regime an attractive interaction is also possible. It has been demonstrated numerically that when the distance between two attractively interacting TCS becomes sufficiently small an incoherent closely packed TCS bound state similar to that observed experimentally in [12] can be formed, This bound state having a similarity with the bound state reported in a Haus master equation model of a ML laser with a slow saturable absorber [22] is weakly oscillating and affected by both the non-local and local interaction. Local interaction, unlike the non-local one, depends strongly on the phase difference of the interacting TCSs. In the case of locally interacting TCSs in a laser with relatively narrow spectral filter in-phase or anti-phase HML regime can develop depending on the value of the pump parameter. Moreover, a bistability between stationary and breathing HML regimes is also possible. Note that the approach presented here is very general and applicable to describe TCS interaction in a wide class of ML lasers, which can be modeled by DDEs of the form (5).

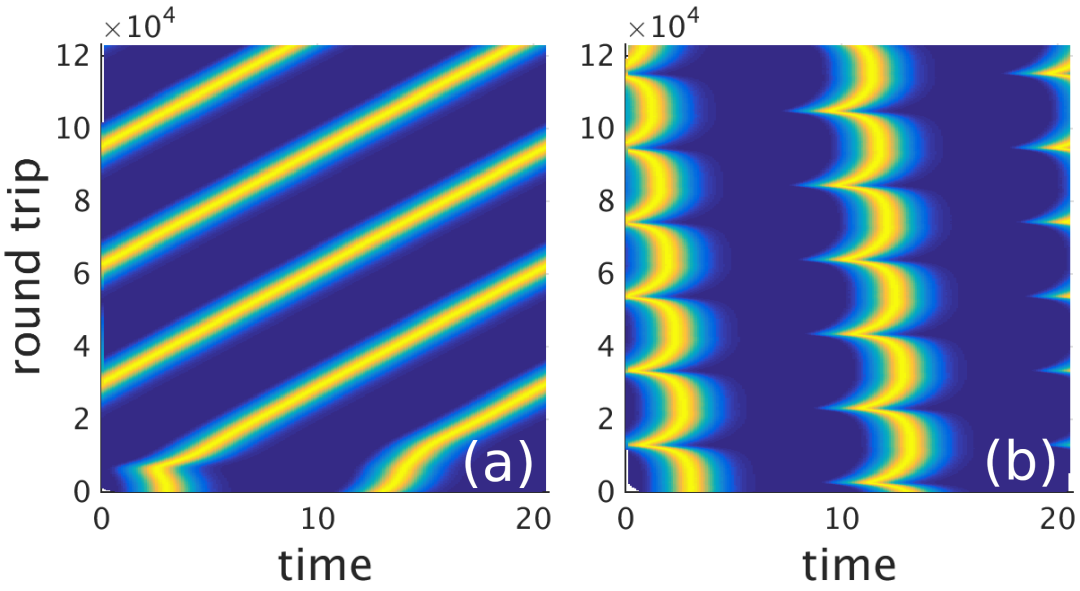

Figure 4: Local TCS interaction leading to a development of stationary bistable anti-phase (a) and breathing (b) HML regimes calculated numerically using different initial conditions. $p = 6.8$, $\tau = 20$, $\gamma = 10$. Other parameters are the same as for Fig. 2.

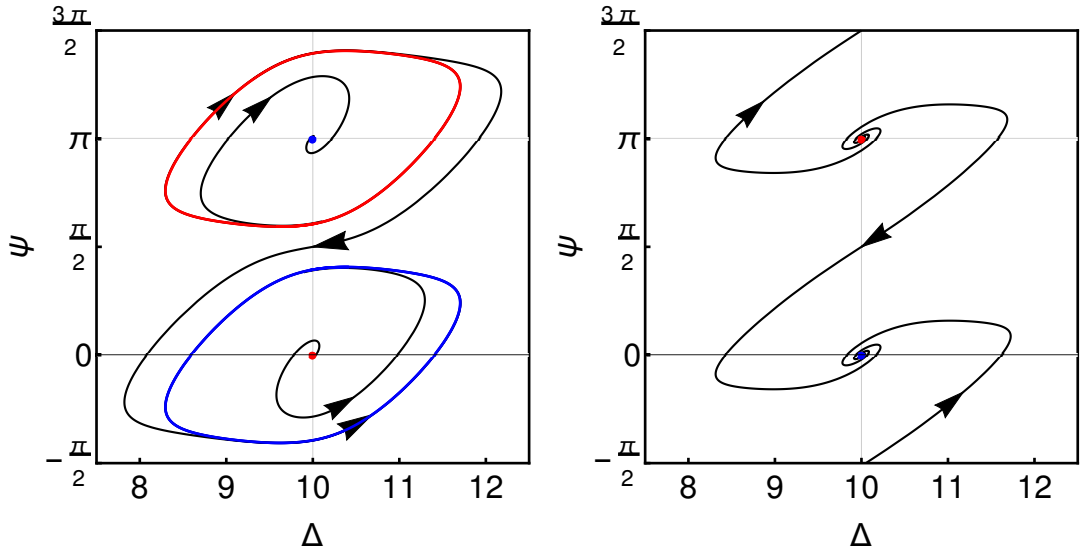

Figure 5: Phase plane of Eqs. (17) and (18) calculated for $p = 6.8$ (a) and $p = 7.2$ (b). Stable (unstable) limit cycle and steady states are shown by blue (red) color. Other parameters are the same as in Fig. 4.

Appendix A Derivation of Eqs. (13) and (14).

Linear operator $\mathcal{L}$ describing the stability of the TCS solution of Eq. (5) and the adjoint operator $\mathcal{L}^\dagger$ are given by:

$$\mathcal{L}\mathbf{v} = -\partial_t \mathbf{v} + \mathcal{B}(t)\boldsymbol{v} + \mathcal{C}(t-\tau)\mathbf{v}_\tau, \tag{19}$$

$$\mathcal{L}^\dagger \mathbf{w} = \partial_t \mathbf{w} + \mathbf{w}\mathcal{B}(t) + \mathbf{w}(t+\tau)\mathcal{C}(t), \tag{20}$$

where $\mathbf{v}$ ($\mathbf{w}$) is a column (row) vector and the matrices $\mathcal{B}$ and $\mathcal{C}$ are obtained by linearization of $\mathbf{F}$ and $\mathbf{H}$ on the TCS solution $\mathbf{U} = \mathbf{u}_0$.

Using the fact that $\mathbf{u}_1$ and $\mathbf{u}_2$ in Eq. (10) are the solutions of Eq. (5) the quantity $\mathbf{P}$ defined by Eq. (12) can be rewritten in the form $\mathbf{P} = \mathbf{Q} + \mathbf{S}(t-\tau)$,where $\mathbf{Q} = \mathbf{F}(\mathbf{u}_\Sigma) - \sum_{k=1}^{2}\mathbf{F}(\mathbf{u}_k)$ and $\mathbf{S} = \mathbf{H}(\mathbf{u}_\Sigma) - \sum_{k=1}^{2}\mathbf{H}(\mathbf{u}_k)$.

Let us for simplicity consider the RHS of the interaction equations for the TCS with the index 2. The RHS of the interaction equation for the first TCS can be obtained in a similar way. Furthermore, to avoid complicating the notation we omit the superscripts τ and ϕ in the adjoint neutral modes. The right hand sides of the interaction equations are then given by

$$\begin{aligned}\langle \mathbf{w}_2\mathbf{P}\rangle &= \langle \mathbf{w}_2[\mathbf{Q} + \mathbf{S}(t-\tau)]\rangle = \langle \mathbf{w}_2\mathbf{Q}\rangle + \langle \mathbf{w}_2(t+\tau)\mathbf{S}\rangle \\ &= \sum_{k=1}^{2}\left[\langle \mathbf{w}_2\mathbf{Q}\rangle_k + \langle \mathbf{w}_2(t+\tau)\mathbf{S}\rangle_k\right],\end{aligned} \tag{21}$$

where I have used τ_0-periodicity of the TCSs and their adjoint neutral modes and split the integral over the interval $[0,\tau_0]$ into two parts $\langle\cdot\rangle = \langle\cdot\rangle_1 + \langle\cdot\rangle_2$ with $\langle\cdot\rangle_1 \equiv \int_0^{\tau_0/2}\cdot dt$ and $\langle\cdot\rangle_2 \equiv \int_{\tau_0/2}^{\tau_0}\cdot dt$. Here without the loss of generality it is assumed that the coordinate origin is located in the middle point between two TCSs, see Fig. 1. Since $\mathbf{u}_1$ is small on the integration interval $[0,\tau_0/2]$, we obtain $\mathbf{Q} \approx (\mathcal{B}_2 - \mathcal{B}_0)\mathbf{u}_1$ and $\mathbf{S} \approx (\mathcal{C}_2 - \mathcal{C}_0)\mathbf{u}_1$ on this interval. Here the linearization matrices $\mathcal{B}_2(t)$ and $\mathcal{C}_2(t)$ are similar to $\mathcal{B}(t)$ and $\mathcal{C}(t)$ in Eqs. (19) and (20), but evaluated on $\mathbf{u}_2$ instead of $\mathbf{u}_0$, while $\mathcal{B}_0$ and $\mathcal{C}_0$ are the linearizations of $\mathbf{F}$ and $\mathbf{H}$ on the trivial solution $\mathbf{U} = 0$. Similarly, on the interval $[\tau_0/2,\tau_0]$ the second TCS $\mathbf{u}_2$ is small and one can write $\mathbf{Q} \approx (\mathcal{B}_1 - \mathcal{B}_0)\mathbf{u}_2$ and $\mathbf{S} \approx (\mathcal{C}_1 - \mathcal{C}_0)\mathbf{u}_2$, where $\mathcal{B}_1(t)$ and $\mathcal{C}_1(t)$ are the matrices $\mathcal{B}(t)$ and $\mathcal{C}(t)$ evaluated on $\mathbf{u}_1$ instead of $\mathbf{u}_0$. Substituting these approximate relations into (21) and neglecting the second order terms containing $\mathbf{w}_2$ and $\mathbf{u}_2$ on the interval $[\tau_0/2,\tau_0]$ yields:

$$\langle \mathbf{w}_2\mathbf{P}\rangle \approx \langle[\mathbf{w}_2(\mathcal{B}_2 - \mathcal{B}_0) + \mathbf{w}_2(t+\tau)(\mathcal{C}_2 - \mathcal{C}_0)]\mathbf{u}_1\rangle_1. \tag{22}$$

Using the relation $\mathcal{L}_2\mathbf{w}_2 = \partial_t\mathbf{w}_2 + \mathbf{w}_2\mathcal{B}_2 + \mathbf{w}_2(t+\tau)\mathcal{C}_2 = 0$, where $\mathcal{L}_2$ is the linear operator $\mathcal{L}$ evaluated on the solution $\mathbf{u}_2$ instead of $\mathbf{u}_0$, one gets

$$\langle \mathbf{w}_2\mathbf{P}\rangle \approx -\langle[\partial_t\mathbf{w}_2 + \mathbf{w}_2\mathcal{B}_0 + \mathbf{w}_2(t+T)\mathcal{C}_0]\mathbf{u}_1\rangle_1.$$

Finally using the relation $\mathcal{L}_0\mathbf{u}_1 = -\partial_t\mathbf{u}_1 + \mathcal{B}_0\mathbf{u}_1 + \mathcal{C}_0\mathbf{u}_1(t-\tau) \approx 0$ on the interval $[0,\tau_0/2]$, where $\mathbf{u}_1$ is small, one obtains

$$\begin{aligned}\langle \mathbf{w}_2\mathbf{P}\rangle \approx -\langle[(\partial_t\mathbf{w}_2)\mathbf{u}_1 + \mathbf{w}_2\partial_t\mathbf{u}_1 + \mathbf{w}_2(t+T)\mathcal{C}_0\mathbf{u}_1 - \mathbf{w}_2\mathcal{C}_0\mathbf{u}_1(t-\tau)]\mathbf{u}_1\rangle_1 = \\ \mathbf{w}_2(0)\mathbf{u}_1(0) - \mathbf{w}_2(\tau_0/2)\mathbf{u}_1(\tau_0/2).\end{aligned} \tag{23}$$

Here the relation $\mathcal{C}_0 = 0$, which is valid for the symmetric splitter, has been used. Similarly to (23), one can get

$$\langle \mathbf{w}_1\mathbf{P}\rangle \approx \mathbf{w}_1(\tau_0/2)\mathbf{u}_2(\tau_0/2) - \mathbf{w}_1(\tau_0)\mathbf{u}_2(\tau_0) = -\mathbf{w}_1(0)\mathbf{u}_2(0) + \mathbf{w}_1(\tau_0/2)\mathbf{u}_2(\tau_0/2). \tag{24}$$

References

[1] M. J. Ablowitz, T. P. Horikis, and S. D. Nixon. Soliton strings and interactions in mode-locked lasers. *Optics communications*, 282(20):4127–4135, 2009.

[2] N. Akhmediev, A. S. Rodrigues, and G. E. Town. Interaction of dual-frequency pulses in passively mode-locked lasers. *Optics communications*, 187(4-6):419–426, 2001.

[3] P. Camelin, J. Javaloyes, M. Marconi, and M. Giudici. Electrical addressing and temporal tweezing of localized pulses in passively-mode-locked semiconductor lasers. *Phys. Rev. A*, 94(6):063854, 2016.

[4] N. Doran and D. Wood. Nonlinear-optical loop mirror. *Opt. Lett.*, 13(1):56–58, 1988.

[5] M. E. Fermann, F. Haberl, M. Hofer, and H. Hochreiter. Nonlinear amplifying loop mirror. *Optics Letters*, 15(13):752–754, 1990.

[6] P. Grelu and N. Akhmediev. Dissipative solitons for mode-locked lasers. *Nature photonics*, 6(2):84–92, 2012.

[7] P. Grelu and J. Soto-Crespo. Multisoliton states and pulse fragmentation in a passively mode-locked fibre laser. *Journal of Optics B: Quantum and Semiclassical Optics*, 6(5):S271, 2004.

[8] A. Halanay and A. Halanay. *Differential equations: Stability, oscillations, time lags*, volume 6. Elsevier, 1966.

[9] T. Herr, V. Brasch, J. D. Jost, C. Y. Wang, N. M. Kondratiev, M. L. Gorodetsky, and T. J. Kippenberg. Temporal solitons in optical microresonators. *Nature Photonics*, 8(2):145–152, 2014.

[10] J. Javaloyes, P. Camelin, M. Marconi, and M. Giudici. Dynamics of localized structures in systems with broken parity symmetry. *Phys. Rev. Lett.*, 116(13):133901, 2016.

[11] T. J. Kippenberg, A. L. Gaeta, M. Lipson, and M. L. Gorodetsky. Dissipative Kerr solitons in optical microresonators. *Science*, 361(6402), 2018.

[12] A. Kokhanovskiy, E. Kuprikov, and S. Kobtsev. Single-and multi-soliton generation in figure-eight mode-locked fibre laser with two active media. *Optics & Laser Technology*, 131:106422, 2020.

[13] J. N. Kutz, B. Collings, K. Bergman, and W. Knox. Stabilized pulse spacing in soliton lasers due to gain depletion and recovery. *IEEE journal of quantum electronics*, 34(9):1749–1757, 1998.

[14] W. J. Lai, P. Shum, and L. Binh. NOLM-NALM fiber ring laser. *IEEE journal of quantum electronics*, 41(7):986–993, 2005.

[15] F. Leo, S. Coen, P. Kockaert, S.-P. Gorza, P. Emplit, and M. Haelterman. Temporal cavity solitons in one-dimensional Kerr media as bits in an all-optical buffer. *Nature Photonics*, 4(7):471, 2010.

[16] X. Liu. Interaction and motion of solitons in passively-mode-locked fiber lasers. *Phys. Rev. A*, 84(5):053828, 2011.

[17] M. Marconi, J. Javaloyes, S. Balle, and M. Giudici. How lasing localized structures evolve out of passive mode locking. *Phys. Rev. Lett.*, 112(22):223901, Jun 2014.

[18] M. Nizette, D. Rachinskii, A. Vladimirov, and M. Wolfrum. Pulse interaction via gain and loss dynamics in passive mode locking. *Physica D: Nonlinear Phenomena*, 218(1):95–104, 2006.

[19] M. Nizette and A. G. Vladimirov. Generalized haus master equation model for mode-locked class-b lasers. *Phys. Rev. E*, 104:014215, July 2021.

[20] J. Peng, S. Boscolo, Z. Zhao, and H. Zeng. Breathing dissipative solitons in mode-locked fiber lasers. *Science advances*, 5(11):eaax1110, 2019.

[21] D. Puzyrev, A. Vladimirov, A. Pimenov, S. Gurevich, and S. Yanchuk. Bound pulse trains in arrays of coupled spatially extended dynamical systems. *Phys. Rev. Lett.*, 119(16):163901, 2017.

[22] J. M. Soto-Crespo and N. Akhmediev. Multisoliton regime of pulse generation by lasers passively mode locked with a slow saturable absorber. *JOSA B*, 16(4):674–677, 1999.

[23] A. Vladimirov, G. Khodova, and N. Rosanov. Stable bound states of one-dimensional autosolitons in a bistable laser. *Phys. Rev. E*, 63(5):056607, 2001.

[24] A. G. Vladimirov, S. V. Gurevich, and M. Tlidi. Effect of cherenkov radiation on localized-state interaction. *Phys. Rev. A*, 97(1):013816, 2018.

[25] A. G. Vladimirov, A. V. Kovalev, E. A. Viktorov, N. Rebrova, and G. Huyet. Dynamics of a class-A nonlinear mirror mode-locked laser. *Phys. Rev. E*, 100(1):012216, 2019.

[26] A. G. Vladimirov, S. Suchkov, G. Huyet, and S. K. Turitsyn. Delay-differential-equation model for mode-locked lasers based on nonlinear optical and amplifying loop mirrors. *Phys. Rev. A*, 104(3):033525, 2021.

[27] A. G. Vladimirov, M. Tlidi, and M. Taki. Dissipative soliton interaction in kerr resonators with high-order dispersion. *Phys. Rev. A*, 103(6):063505, 2021.

[28] A. G. Vladimirov and D. Turaev. New model for mode-locking in semiconductor lasers. *Radiophys. & Quant. Electron.*, 47(10-11):857–865, 2004.

[29] A. G. Vladimirov and D. Turaev. Model for passive mode locking in semiconductor lasers. *Phys. Rev. A*, 72(3):033808, 2005.

[30] A. G. Vladimirov, D. Turaev, and G. Kozyreff. Delay differential equations for mode-locked semiconductor lasers. *Opt. Lett.*, 29:1221–1223, 2004.

[31] Z. Wang, K. Nithyanandan, A. Coillet, P. Tchofo-Dinda, and P. Grelu. Optical soliton molecular complexes in a passively mode-locked fibre laser. *Nature communications*, 10(1):1–11, 2019.

[32] S. Yanchuk, S. Ruschel, J. Sieber, and M. Wolfrum. Temporal dissipative solitons in time-delay feedback systems. *Physical review letters*, 123(5):053901, 2019.

[33] A. Zaviyalov, P. Grelu, and F. Lederer. Impact of slow gain dynamics on soliton molecules in mode-locked fiber lasers. *Optics letters*, 37(2):175–177, 2012.